Supplementary Information (SI) for EES Solar.
This journal is © The Royal Society of Chemistry 2025

Supporting Information

High Coordination-Solvent Bathing for Efficient Crystallization of MA-free Triple Halide Perovskite Solar Cells

José J. Jerónimo-Rendon,[a] Somayeh Gholipour,*[a,b] Sofya Svetlosanova,[a] Rajarshi Roy,[a] Stephan Boehringer,[a] Seyma Topcu,[a] Weiwei Zuo,[a] Mohammadreza Zohdi,[a] Mojtaba Ataei,[a] Mayank Kedia,[a,b] Anna Zhuravlova,[c] Silver-Hamill Turren-Cruz,[d,e] Paolo Samorì,[c] Antonio Gaetano Ricciardulli,[c] Mahdi Malekshahi Byranvand,*[a,b] and Michael Saliba*[a,b]

[a] Institute for Photovoltaics (ipv), University of Stuttgart, Stuttgart D-70569, Germany, Email : somayeh.gholipour@ipv.uni-stuttgart.de, mahdi.malekshahi-byranvand@ipv.uni-stuttgart.de, michael.saliba@ipv.uni-stuttgart.de
[b] Helmholtz Young Investigator Group FRONTRUNNER, IEK5-Photoevoltaik, Forschungszentrum, Jülich 52425, Germany
[c] Université de Strasbourg, CNRS, ISIS 8 Allée Gaspard Monge, Strasbourg 67000, France
[d] Department of Physical Chemistry, Polish Academy of Sciences, Warsaw 01-224, Poland
[e] Instituto de Ciencia de los Materiales (ICMUV), Universitat de Valencia, 46980 Paterna, Spain

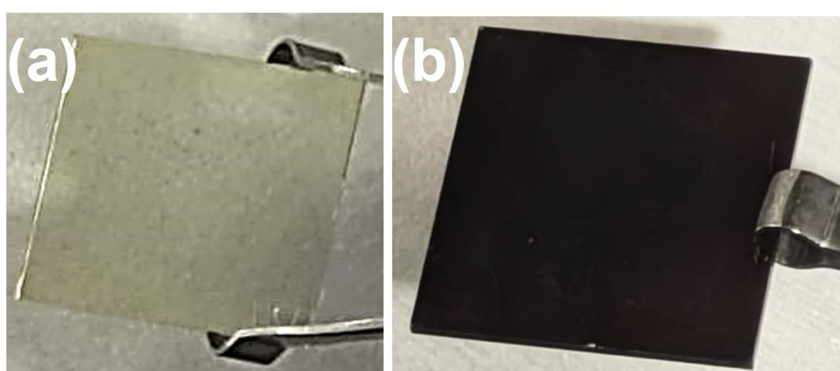

Fig. S1. The 3-hal Perovskite films formed by the ASB approach before (a) and after (b) submerging in DMS solvent.

Table S1. A summary of the absorbance onset, and PL peak for different annealing temperatures estimated from UV-vis, and steady-state PL spectra are reported in Fig. 1b, and c, respectively.

annealing condition	UV-vis onset (nm)	PL peak (nm)
Ref	752.03	743.0
AT25	777.49	771.2
AT40	776.2	761.7

AT60	767.49	757.0
AT80	756.52	743.4
AT100	767.48	756.4

Carrier lifetime measurements from TRPL analysis

The PL decay lifetime was obtained by fitting the TRPL spectra measured from the perovskite films with a biexponential decay function for the reference sample and perovskite layers with different annealing temperatures:

$$I(t) = A_1\, exp\left(-\frac{t}{\tau_1}\right) + A_2\, exp\left(-\frac{t}{\tau_2}\right) + K \tag{S1}$$

where A1 and A2 are the decay amplitude, τ_1 and τ_2 are the decay time and K is a constant for the base-line offset. The average PL decay times (τavg) are further estimated using the following expression:

$$\tau_{avg} = \frac{A_1\tau_1^2 + A_2\tau_2^2}{A_1\tau_1 + A_2\tau_2} \tag{S2}$$

Table S2. A summary of the carrier lifetime estimated from fitting TRPL spectra for different annealing temperatures is reported in Fig. 2d.

annealing condition	τ_1 **(ns)**	A_1 **(%)**	τ_2 **(ns)**	A_2 **(%)**	τ_{avg} **(ns)**
Ref	37.89	0.42	576.13	0.58	551.42
AT25	54.80	0.48	251.27	0.52	218.46

AT40	15.53	0.84	601.19	0.16	531.78
AT60	31.49	0.44	1017.55	0.56	993.76
AT80	13.50	0.67	1076.07	0.33	1049.48
AT100	27.03	0.60	352.60	0.40	319.25

Methods for calculating carrier mobility, defect density, and diffusion length

The electron mobility and defect densities in the perovskite device were predicted by fabricating an electron-only device with a structure of ITO/compact-SnO_2/perovskite/PC61BM/Au. The *J*-*V* response of the device was then recorded in the dark under an ambient atmosphere collected by Keithley 2400. The double logarithmic plot of the result will contain a linear and a quadratic dependence of J over the applied bias V and a trap-filling transition (TFL). The linear one is the Ohmic response of the device. Trap density determines the voltage:

$$V_{TFL} = \frac{e n_{trap} L^2}{2\varepsilon_r \varepsilon_0} \quad \text{(S3)}$$

which at all traps are filled, where e = 1.602×10^{-19} C is the elemental charge, n_{trap} is the electron trap density, L is the thickness of the film, $\varepsilon_0 = 8.854\times10^{-14}$ F cm^{-1} is the vacuum permittivity, ε_r is the relative dielectric constant.[1]

The quadratic part is the space-charge limited current characteristic of the device, which is well-described using a Mott-Gurney relation of:

$$J = \frac{9\varepsilon_r \varepsilon_0 \mu V^2}{8L^3} \quad \text{(S4)}$$

where V, L, m, ε_0, and ε_r are the applied voltage, carrier mobility, vacuum permittivity, and the relative dielectric constant of perovskite, respectively.[2] The Moot-Gurney relation can be simplified as $J = bV^2$, with b = $\frac{9\varepsilon_r\varepsilon_0\mu}{8L^3}$, which is obtained from second-order polynomial fitting of the quadratic part of the curve. According to the literature, the dielectric constant ε_r of perovskite is determined to be 46.9.[3] The thickness of reference perovskite film was 730 nm, and the films deposited by the ASB method, annealed at different temperatures of 25, 40, 60, 80 and 100 ºC measured at ~ 650, 660, 680, 715, and 705 nm, respectively which was verified by profilometry.

In addition, free carrier concentration can be calculated using the relation:

$$n_c = \frac{\sigma}{e\mu} \tag{S3}$$

where σ is the conductivity extracted from the ohmic region of the *J-V* curve.

The carrier diffusion length was calculated from the relation:

$$L_D = \sqrt{\frac{\mu\tau k_B T}{e}} \tag{S4}$$

where kB is the Boltzmann's constant, T is the absolute temperature and τ is the carrier lifetime.

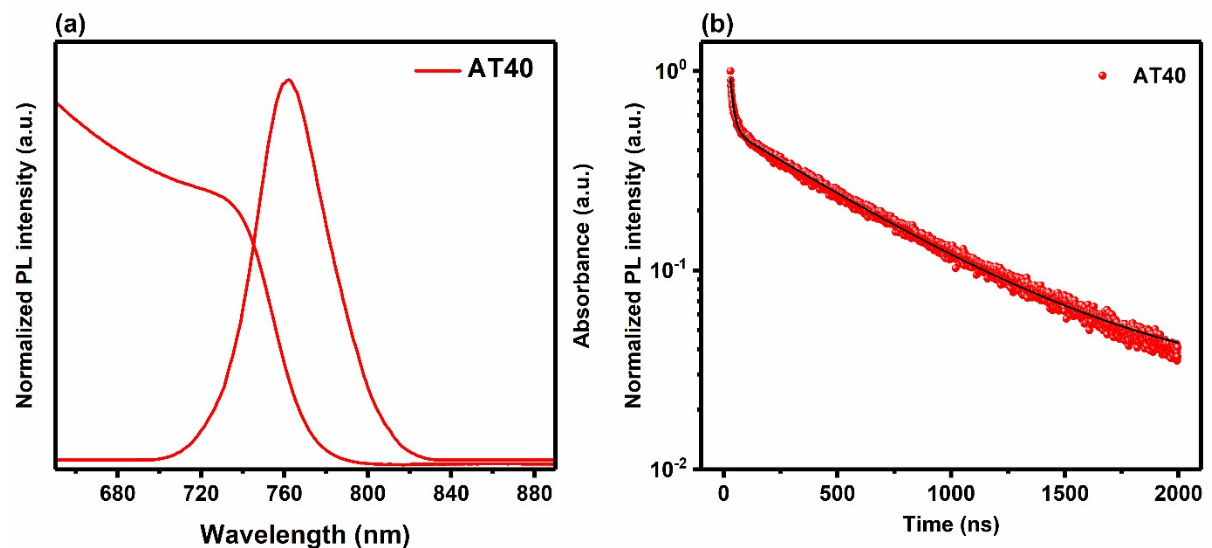

Fig. S2. a) UV-vis, and steady-state photoluminescence (PL), and b) time-resolved photoluminescence (TRPL) spectra for perovskite films annealed at 40 °C temperature, which is fabricated by using DMS as high coordination solvent in the ASB approach.

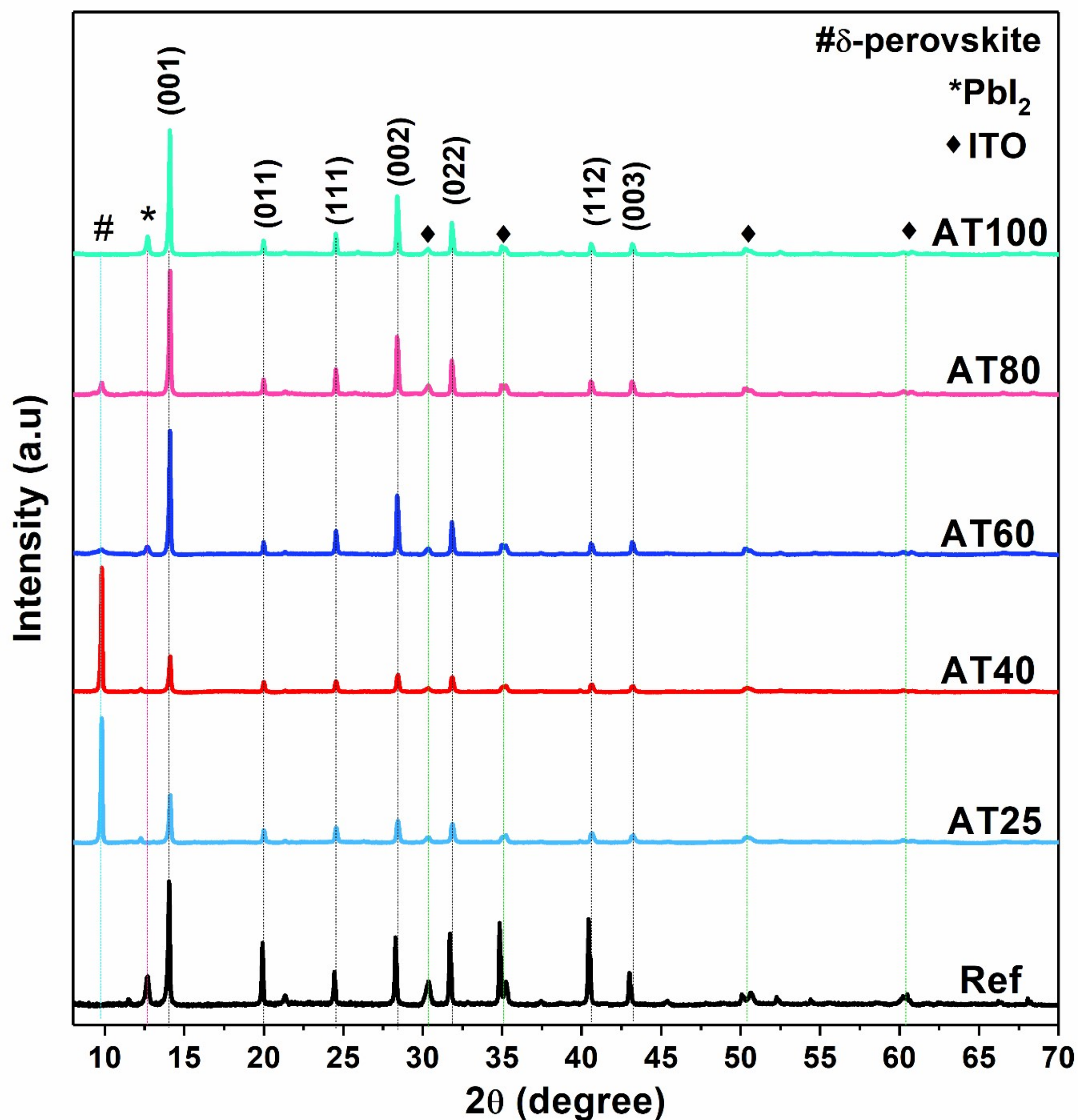

Fig. S3. The XRD pattern for reference sample and 3-hal perovskite films grown on ITO/compact-SnO_2 substrates with different annealing temperatures. Peaks are labeled to denote the perovskite δ-phase (#), cubic PbI_2 (*), and ITO (♦).

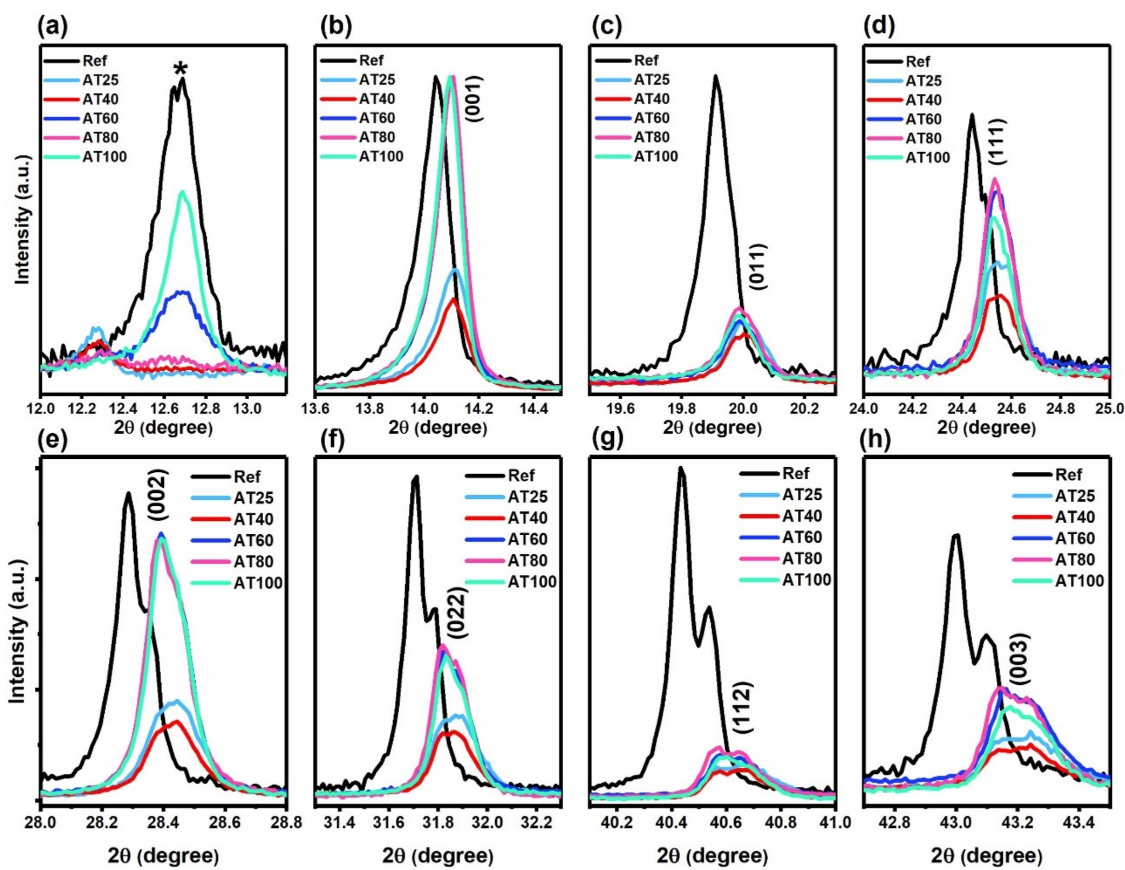

Fig. S4. Magnified XRD pattern for a) PbI_2, b) (001), c) (011), d) (111), e) (002), f) (022), g) (112), and h) (003) diffraction peaks.

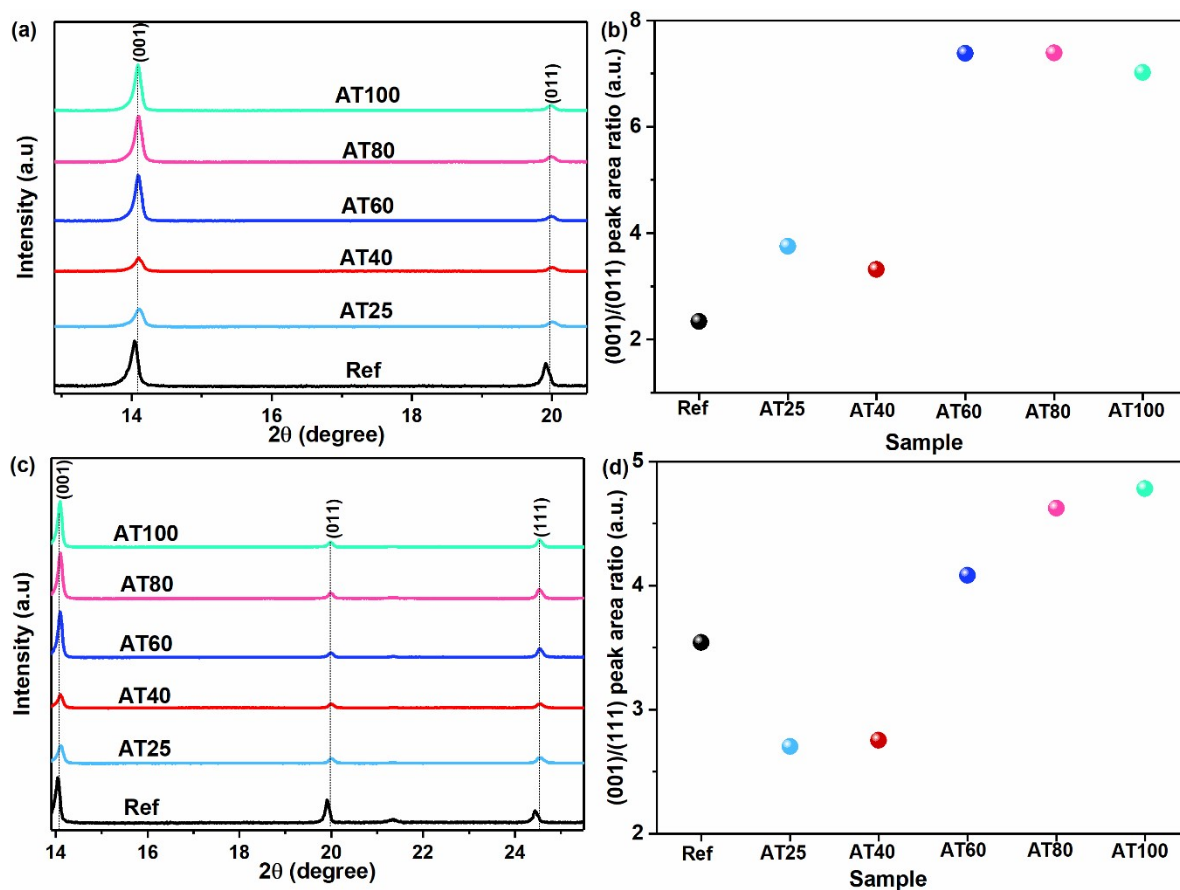

Fig. S5. a), c) Magnified XRD pattern for (001), (011), and (111) peaks, for the reference sample and 3-hal perovskite films grown on ITO/compact-SnO_2 substrates with different annealing temperatures, b) the (001) to (001) peak area ratio, and d) the (001) to (111) peak area ratio at different annealing temperatures.

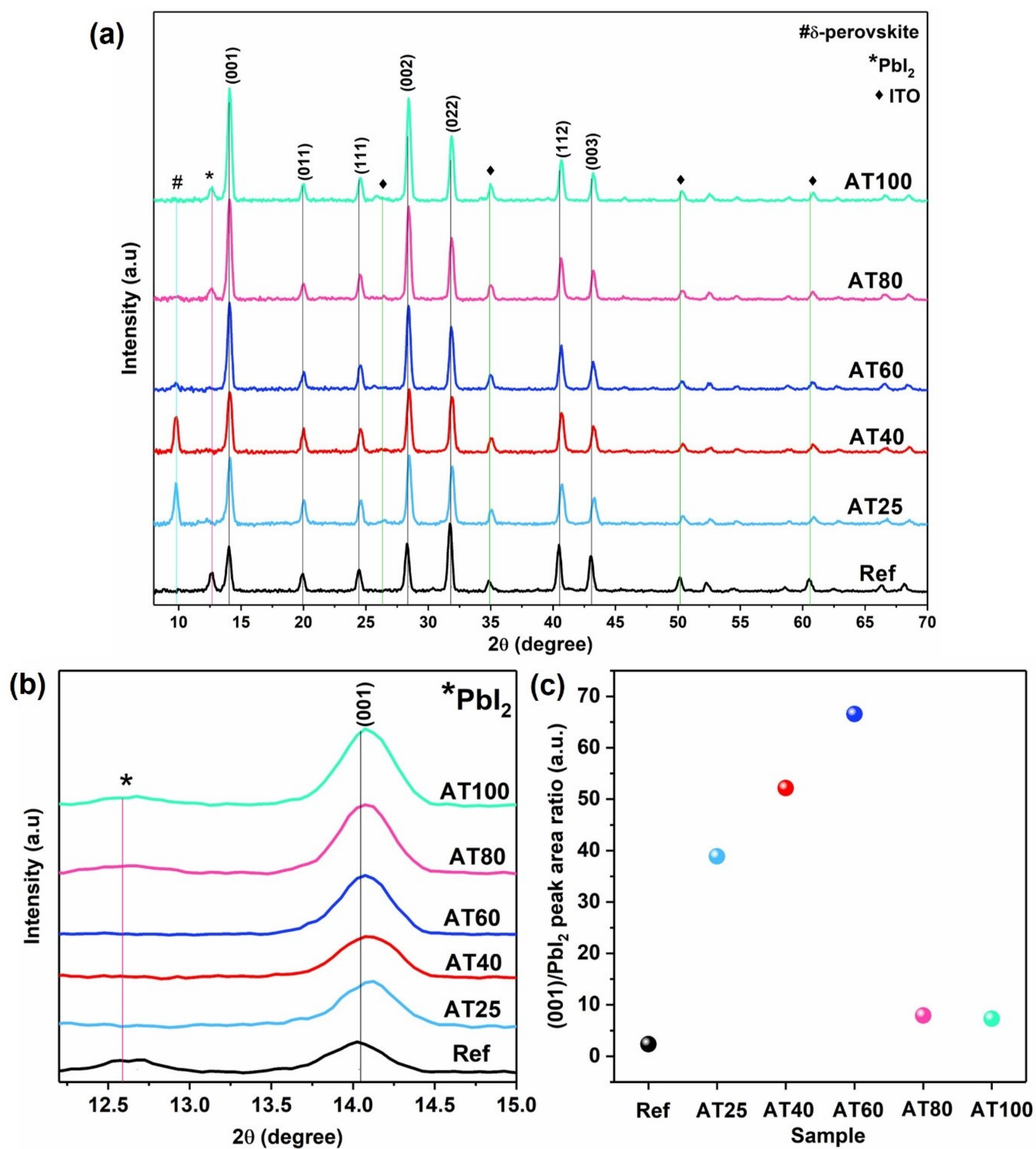

Fig. S6. a) The XRD pattern (surface) for reference sample and 3-hal perovskite films grown on ITO/compact-SnO_2 substrates with different annealing temperatures. Peaks are labeled to denote the perovskite δ-phase (#), cubic PbI_2 (*), and ITO (♦), b) Magnified XRD pattern (surface) for PbI_2 (*), and (001) peaks, c) the (001) to PbI_2 peak area ratio, at different annealing temperatures.

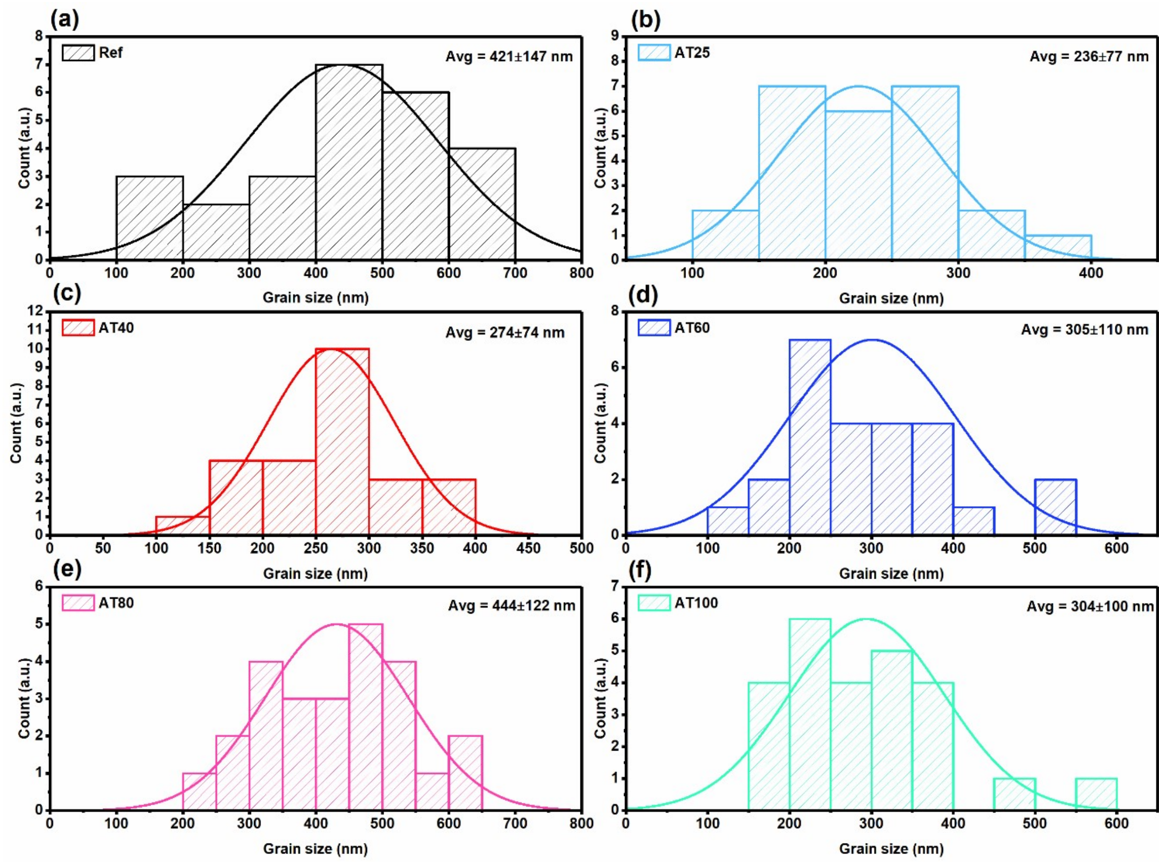

Fig. S7. Statical grain size distribution for the a) reference perovskite film, and the perovskite layers fabricated by the ASB method at different annealing temperatures of b) 25, b) 40, c) 60, d) 80 and d)100 ºC.

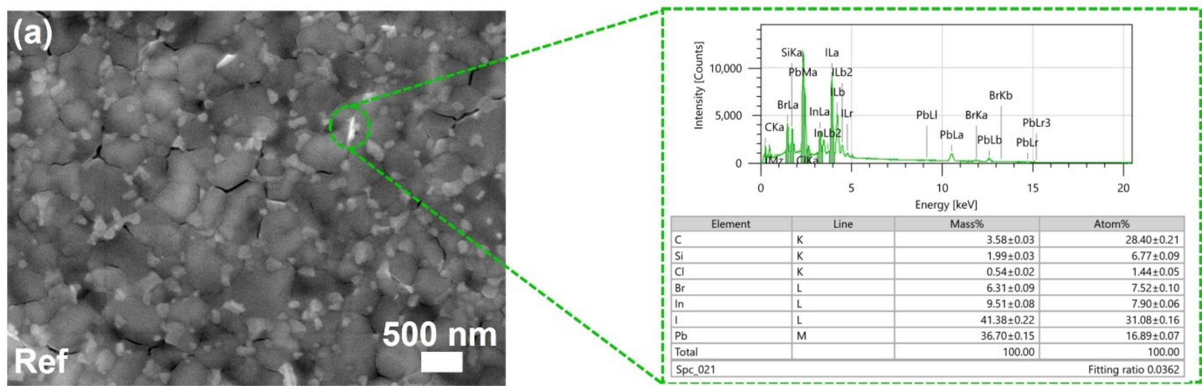

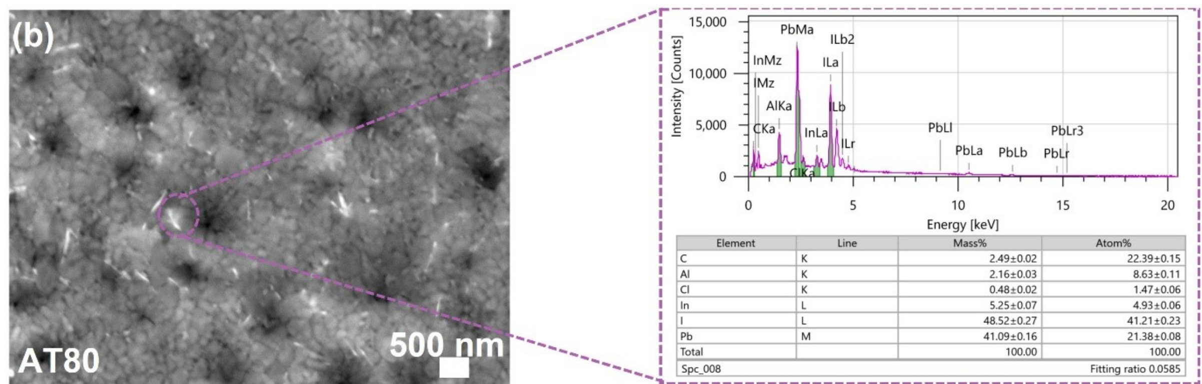

Fig. S8. EDX analysis of the a) reference film, and b) the ASB-based perovskite films annealed at 80 ºC.

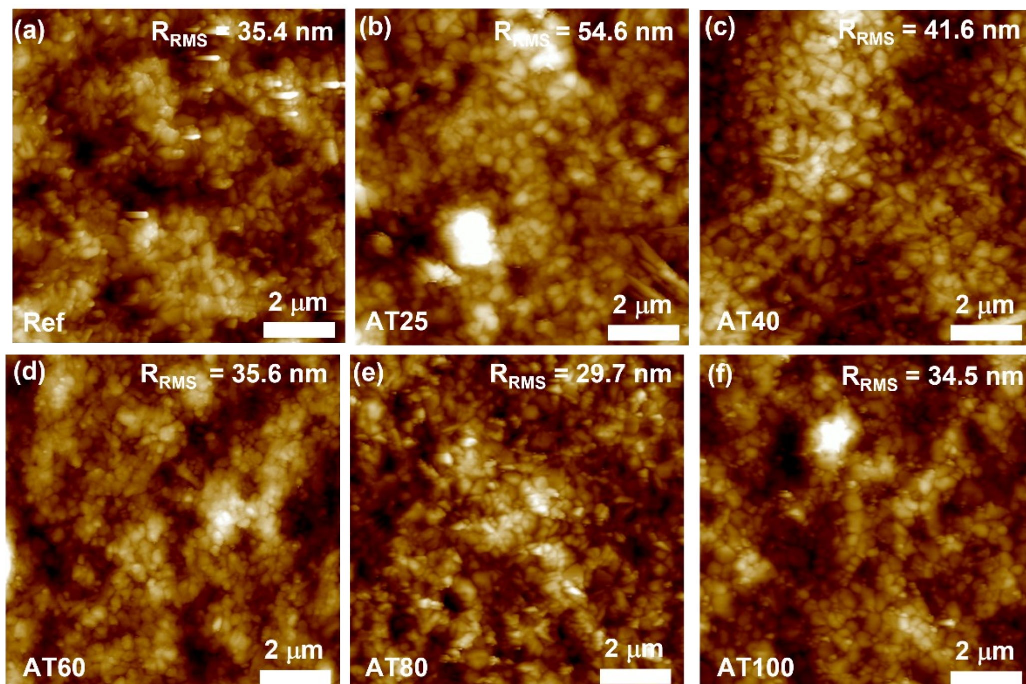

Fig. S9. AFM images of reference and the ASB-based perovskite films annealed at different temperatures. RRMS stands for root mean square of film roughness.

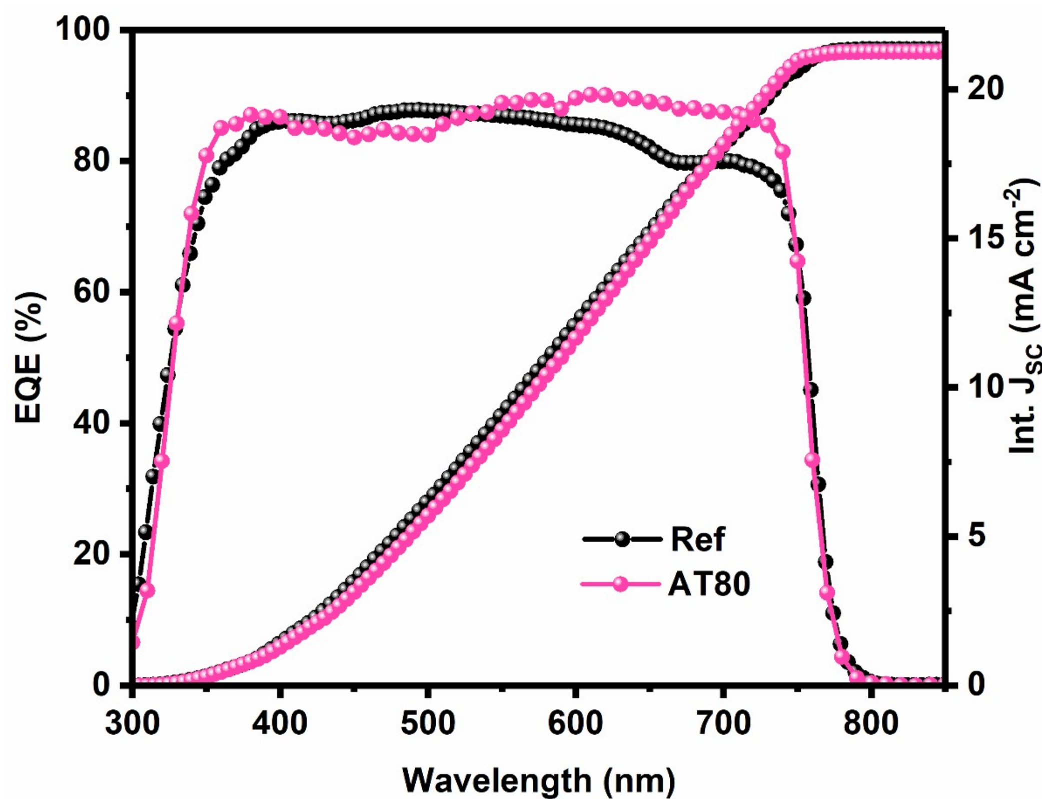

Fig. S10. EQE spectrum and integrated JSC of the reference and the AT80-based PSCs.

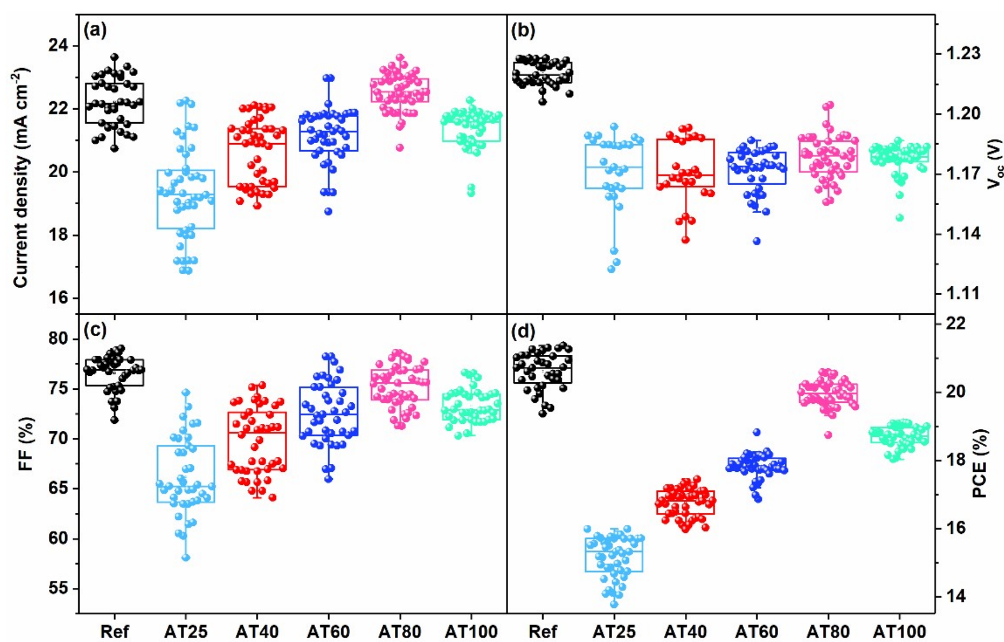

Fig. S11. Statistical PV parameters including a) VOC, b) J_{SC}, c) FF, and d) PCE, for PSCs fabricated with perovskite films at different annealing temperatures.

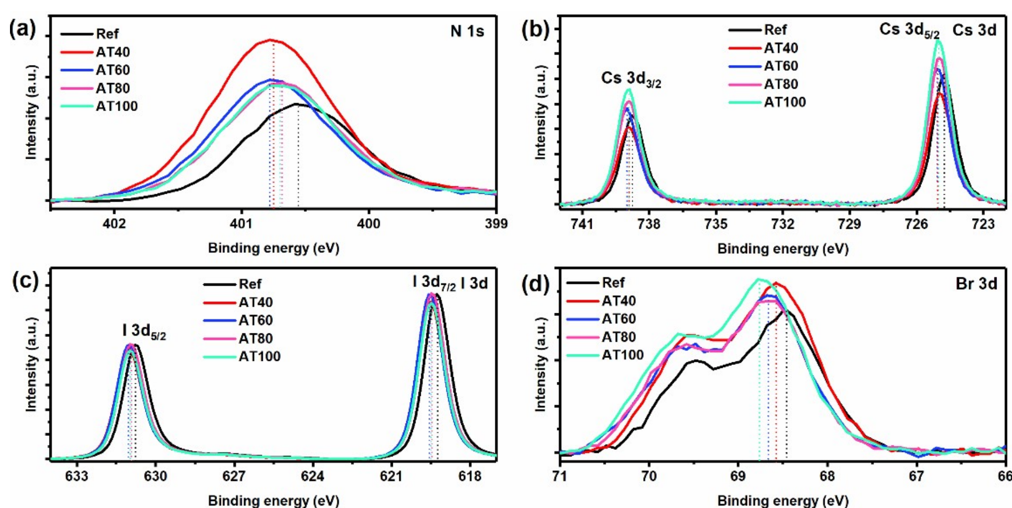

Fig. S12. The XPS spectra of the (a) N 1s, (b) Cs 3d, (c) I 3d, and (d) Br 3d regions of the reference sample and perovskite layers with different annealing temperatures.

References

1 J. H. Heo, M. S. You, M. H. Chang, W. Yin, T. K. Ahn, S.-J. Lee, S.-J. Sung, D. H. Kim and S. H. Im, *Nano Energy*, 2015, **15**, 530–539.
2 C.-H. Chiang and C.-G. Wu, *Nature Photon*, 2016, **10**, 196–200.
3 Q. Yang, X. Liu, S. Yu, Z. Feng, L. Liang, W. Qin, Y. Wang, X. Hu, S. Chen, Z. Feng, G. Hou, K. Wu, X. Guo and C. Li, *Energy Environ. Sci.*, 2021, **14**, 6536–6545.